Supporting information

Developing phenanthroimidazole-based host materials with balanced hole-electron transport feature for highly efficient blue fluorescent OLED

Zhiqiang Wang, [a] *Bohua Zhang,* [b] *Yi Chen,* [b] *Jiangxue Pei,* [b], *Qingyu Jia,* [b] *Chaobo Hao,* [b] *Xiping Lei* [*a] *and Dongdong Wang*[*b]

[a] *College of Materials Science and Engineering, Xi'an University of Architecture and Technology, xi'an 710055 P.R. China.*
[b] *School of Chemistry, Xi'an Jiaotong University, Xi'an 710049, P. R. China.*
c Key Laboratory of Physical Electronics and Devices of Ministry of Education & Shaanxi Key Laboratory of Information Photonic Technique, School of Electronic Science and Engineering, Xi'an Jiaotong University, Xi'an 710049, China.

Corresponding author:
Xiping Lei
E-mail: sxxhyleixiping@163.com
Dongdong Wang
E-mail: ddwang@mail.xjtu.edu.cn

Contents

S1. General information

Unless otherwise stated, all chemicals and materials are already available on the market and can be used without further purification. All solvents used for reaction and photophysical measurements are HPLC-grade solvents. TGA-DSC measurements from room temperature to 800 °C were made using the Shimadzu DTG-60 instrument in a dry nitrogen stream at a heating rate of 10 °C min^{-1}. Cyclic voltammetry (CV) was recorded at a scanning rate of 100 mV s^{-1} on CHI660E electrochemical station of The Shanghai Chenhua Company. 0.1 M tetrabutylammonium perfluorinated phosphorate ($TBAPF_6$) was used as the supporting electrolyte in dried CH_2Cl_2. The conventional three-electrode system consists of glass carbon working electrode, platinum wire auxiliary electrode and Ag/AgCl standard electrode used as reference electrode. The UV-vis absorption spectra of the solution were recorded on the Hitchi 3010 spectrometers. The steady-state and transient fluorescence spectra were measured on the FLS 980 fluorescence spectrometer, and PLQY was measured using the integrating sphere combined with the FLS 980 fluorescence spectrophotometer.

S2. Synthesis and characterization.

All solvents and reagents were purchased from commercial sources and used as received without further purification. The synthetic routes of the target compounds are outlined as below.

(1) The synthetic of *2-(4-bromophenyl)-1-phenyl-1H-phenanthro[9,10-d]imidazole* (PPIBr).

Place phenanthrene-9,10-dione (5 g, 24 mmol), 4-bromobenzaldehyde (4.44 g, 24 mmol) and aniline (8.94 g, 96 mmol) in a dry three-port flask, displace the air with nitrogen, then add NH_4OAc (11.11 g, 144 mmol), followed by the solvent 134 ml AcOH and 134 ml deionized water. Reflux reaction of the mixed solution under nitrogen atmosphere. After detecting the reaction completely with TLC plates, the mixture is cooled and filtered, and then extracted with methylene chloride. The solvent is evaporated under reduced pressure to obtain organic solid. The organic solid was purified by column chromatography and white solid was obtained. ^1H NMR (400 MHz, DMSO-d6) δ 8.87 (m, 2H), 8.65 (m, 1H), 7.76 - 7.72 (m, 1H), 7.71 - 7.63 (m, 6H), 7.55 - 7.50 (m, 3H), 7.49 - 7.45 (m, 2H), 7.34 - 7.27 (m, 1H), 7.04 (m, 1H). HRMS(ESI) calculated for $C_{27}H_{17}N_2Br$ $[M+H]^+$ 449.0647, found: 449.0641.

(2) The synthetic of *9-(4-(6-bromodibenzo[b,d]furan-4-yl)phenyl)-9H-carbazole* (Cz-DBFBr,2a).

4,6-dibromodibenzo [b,d]furan (1.14 g, 3.50 mmol), (4-(9H-carbazol-9-yl)phenyl)boronic acid (1 g, 3.5 mmol)and K_2CO_3 (2.42 g, 17.5 mmol)were added to a dry three-port flask, air is replaced with nitrogen, followed by solvent 1,4-Dioxane (60 ml) and deionized water (9 ml). Reflux reaction of the mixed solution under nitrogen atmosphere. After detecting the reaction completely with TLC plates, the mixture is cooled and filtered, and then extracted with methylene chloride. The solvent is evaporated under reduced pressure to obtain organic solid. The organic solid was purified by column chromatography and white solid was obtained. ^1H NMR (400 MHz, DMSO-d6) δ 8.33 - 8.19 (m, 6H), 7.93 - 7.83 (m, 3H), 7.81 (d, J = 8.2 Hz, 1H), 7.59 (m, 2H), 7.55 - 7.43 (m, 5H), 7.37 - 7.30 (m, 2H).

(3) The synthetic of *4-(6-bromodibenzo[b,d]furan-4-yl)-N,N-diphenylaniline* (TPA-DBFBr,2b).

Add 4,6-dibromodibenzo [b,d]furan (1 g, 3.07 mmol), (4-(diphenylamino) phenyl) boronic acid (0.89 g, 3.07 mmol) and K_2CO_3 (2.12 g, 15.35 mmol) to a dry three-port flask, displace the air with nitrogen, then add the solvent 1,4-Dioxane (60 ml) and deionized water (8 ml). Reflux reaction of the mixed solution under nitrogen atmosphere. After detecting the reaction completely with TLC plates, the mixture is cooled and filtered, and then extracted with methylene chloride. The solvent is evaporated under reduced pressure to obtain organic solid. The organic solid was purified by column chromatography and

white solid was obtained. ^{1}H NMR (400 MHz, DMSO-d6) δ 8.20 (d, *J* = 7.6 Hz, 1H), 8.13 (d, *J* = 7.7 Hz, 1H), 7.91 (d, *J* = 8.6 Hz, 2H), 7.76 (d, *J* = 7.7 Hz, 2H), 7.52 (m, 1H), 7.40 - 7.31 (m, 5H), 7.12 (m, 8H).

(4) The synthetic of *4,6-bis(4-(1-phenyl-1H-phenanthro[9,10-d]imidazol-2-yl)phenyl)dibenzo[b,d]furan* (DPPI-DBF). 4,6-dibromodibenzo[b,d]furan (0.31 g, 0.95 mmol), 1-phenyl-2-(4-(4,4,5,5-tetramethyl-1,3,2-dioxaborolan-2-yl)phenyl)-1H-phenanthro[9,10-d] imidazole (1 g, 2.00 mmol) and K_2CO_3 (0.66 g, 4.75 mmol)are added to a dry three-port flask, air is replaced with nitrogen, followed by solvent tetrahydrofuran (THF)(60 ml) and deionized water (3 ml). Reflux reaction of the mixed solution under nitrogen atmosphere. After detecting the reaction completely with TLC plates, the mixture is cooled and filtered, and then extracted with methylene chloride. The solvent is evaporated under reduced pressure to obtain organic solid. The organic solid was purified by column chromatography to obtain the green solid. ^{1}H NMR (400 MHz, DMSO-d6) δ 8.92 (m, 4H), 8.81 (d, J = 7.1 Hz, 2H), 8.23 (d, J = 7.7 Hz, 2H), 8.02 (d, J = 8.4 Hz, 4H), 7.85 - 7.81 (m, 6H), 7.78 (d, J = 8.4 Hz, 5H), 7.76 - 7.67 (m, 8H), 7.62 (m, 2H), 7.55 (m, 4H), 7.33 (m, 2H), 7.08 (d, J = 8.3 Hz, 2H). ^{13}C NMR (151 MHz, Chloroform-d) δ 153.21, 130.52, 130.34, 129.81, 129.50, 129.06, 128.50, 128.37, 127.61, 126.79, 126.53, 124.95, 124.63, 124.15, 123.56, 123.16, 121.00, 120.25, 29.72. HRMS(ESI) calculated for $C_{66}H_{40}N_4O$ $[M+H]^+$ 905.3274, found: 905.3261.

(5) The synthetic of *2-(4-(6-(4-(9H-carbazol-9-yl)phenyl)dibenzo[b,d]furan-4-yl)phenyl)-1-phenyl-1H-Phenanthrol[9,10-d]imidazole* (Cz-PPI-DBF).

Add **2a** (0.50 g, 1 mmol), PPIBpin(0.50 g, 1 mmol) and K_2CO_3 (0.69 g, 5 mmol) to a dry three-hole round-bottomed flask, purge the air with nitrogen gas, and subsequently introduce solvents toluene (60 ml) under a nitrogen atmosphere. The temperature was elevated to achieve reflux conditions, followed by detection of the reaction using a TLC plate. After cooling the mixture to room temperature, water was added for quenching purposes. Subsequently, the resulting solution was extracted with methylene chloride. Solid organic material was obtained through evaporation of the solvent under reduced pressure. The solid organic matter underwent purification via column chromatography and recrystallization to obtain white products. ^{1}H NMR (400 MHz, DMSO-d6) δ 8.88 (m, 2H), 8.67 (d, *J* = 8.2 Hz, 1H), 8.35 (d, *J* = 7.8 Hz, 2H), 8.28 (m, 4H), 8.07 (d, *J* = 8.2 Hz, 2H), 7.93 (d, *J* = 7.6 Hz, 1H), 7.86 (d, *J* = 7.6 Hz, 1H), 7.83 - 7.72 (m, 5H), 7.68 (m, 1H), 7.65 - 7.59 (m, 5H), 7.59 - 7.48 (m, 4H), 7.33 (m, 2H), 7.27 (m, 1H), 7.14 (m, 2H), 6.85 (d, *J* = 8.3 Hz, 1H), 6.71 (m, 1H). ^{13}C NMR (151 MHz, Chloroform-d) δ 153.16, 147.67, 147.43, 130.45, 130.18, 129.44, 129.32, 129.06, 128.40, 126.63, 126.48, 126.17, 125.14, 124.40, 124.21, 123.81, 123.54, 123.46, 123.13, 120.96, 120.27, 119.29, 29.73. HRMS(ESI) calculated for $C_{57}H_{35}N_3O$ $[M+H]^+$ 778.2852, found: 778.2854.

(6) The synthetic of *N,N-diphenyl-4-(6-(4-(1-phenyl-1H-phenanthro[9,10-d]imidazol-2-yl)phenyl)dibenzo[b,d]furan-4-yl)aniline* (TPA-PPI-DBF).

Add **2b** (0.60 g, 1.23 mmol), PPIBpin(0.61 g, 1.23 mmol) and K_2CO_3 (0.85 g, 6.15 mmol), Using the same method as **Cz-PPI-DBF**, the white target product is obtained.^{1}H NMR (400 MHz, DMSO-d6) δ 8.93 (m, 8.4 Hz, 2H), 8.75 (d, *J* = 8.0 Hz, 1H), 8.22 (d, *J* = 7.8 Hz, 1H), 8.17 (d, *J* = 7.5 Hz, 1H), 8.03 (d, *J* = 8.1 Hz, 2H), 7.92 (d, *J* = 8.5 Hz, 2H), 7.82 (m, 2H), 7.78 - 7.69 (m, 6H), 7.55 (m, 6H), 7.36 (m, 5H), 7.22 - 7.12 (m, 6H), 7.05 (m, 3H). ^{13}C NMR (151 MHz, Chloroform-d) δ 140.87, 138.62, 137.16, 136.53, 135.17, 130.15, 129.99, 129.80, 129.41, 128.98, 128.34, 127.33, 127.08, 126.75, 126.39, 126.28, 126.23, 125.71, 125.03, 124.98, 124.92, 124.63, 124.07, 123.69, 123.65, 123.52, 123.08, 122.94, 120.81, 120.52, 120.28, 110.05, 29.73. HRMS(ESI) calculated for $C_{57}H_{37}N_3O$ $[M+H]^+$ 780.3009, found: 780.2991.

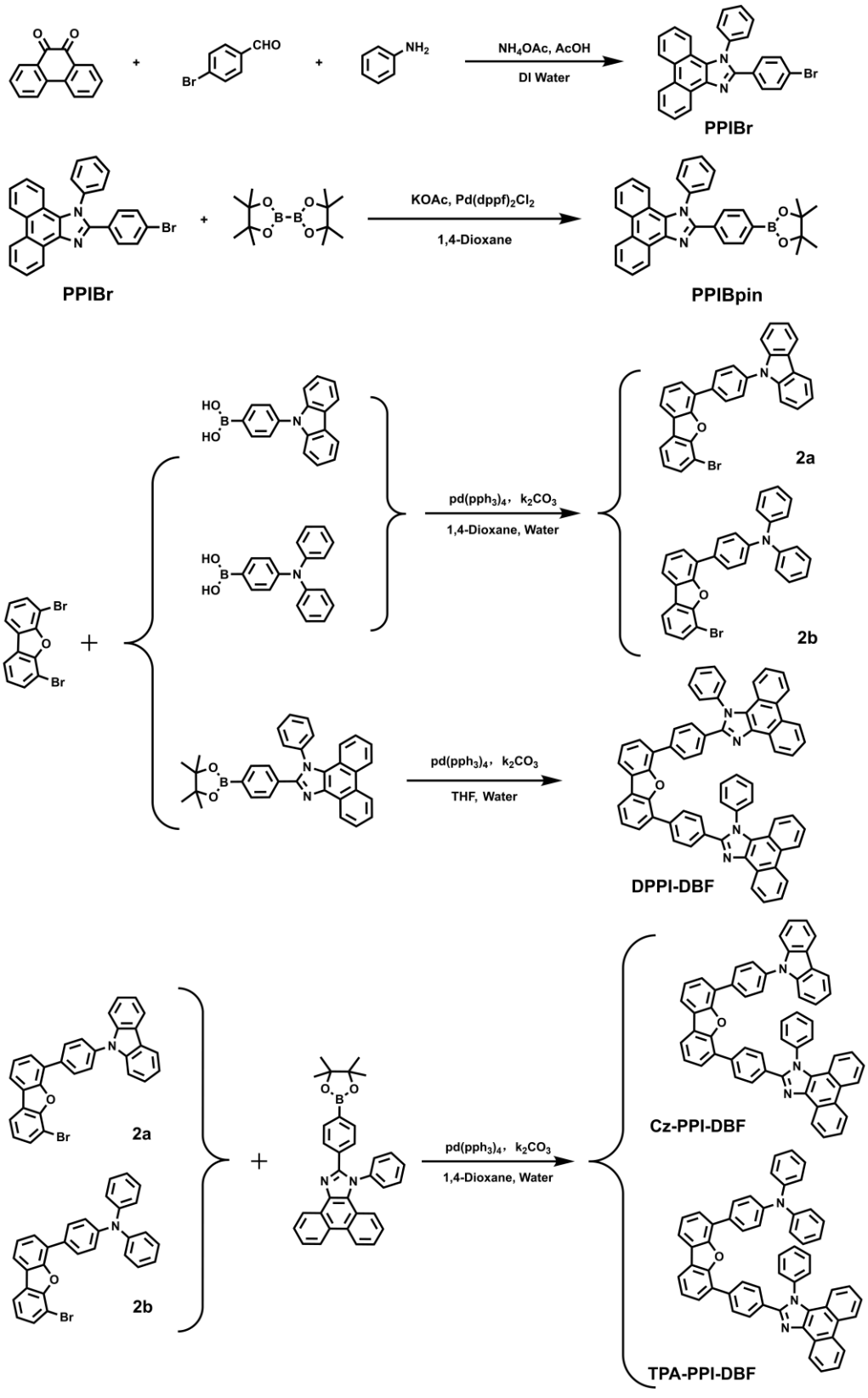

Scheme S1. Synthetic routes and molecular structure of DPPI-DBF, Cz-PPI-DBF and TPA-PPI-DBF.

S3. Computational Methods

All calculations were performed using the Gaussian 09 program package.[1] The ground state geometries were optimized via DFT calculations at the B3LYP / 6-31G(d) level in vacuum. Based on the optimized ground state, the lowest excited singlet state (S_1) and lowest triplet states (T_1) configurations are optimized using the TD-DFT method at the PBE0/6-31G(d) level. Spin-orbit coupling matrix elements (SOCMEs) are gained using the TD-PBE0/TZVP[2] method with the zero-order regular approximation(ZORA)[3] as implemented in the ORCA 4.2.1 program.[4]

S4.Device fabrication and characterization

All the organic layers were successively deposited by means of vacuum deposition onto the ITO-coated glass substrates, which were previously etched, patterned, and washed with detergent, deionized water, acetone, and ethanol in turn. For the doped layer, the dopant and host materials were co-evaporated and the doping concentrations was controlled by deposition rates. The electroluminescence (EL) spectra and CIE coordinates of the devices were measured by a spectrometer (PR650) and the current voltage-luminescence characteristics were analyzed using Keithley 2400 source meter with PR650.

S5. Supplemental Figures and Tables

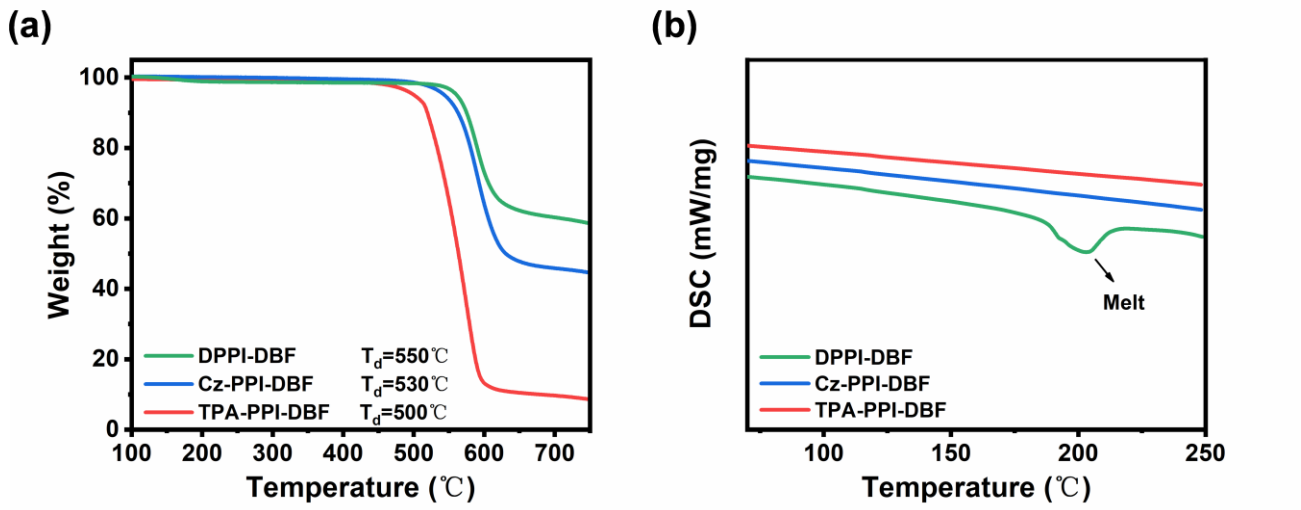

Figure S1. TGA (a) and DSC (b) thermograms of DPPI-DBF, Cz-PPI-DBF and TPA-PPI-DBF.

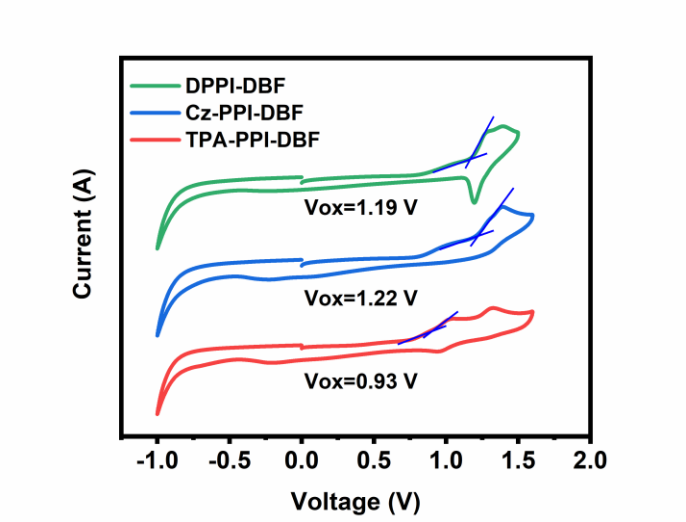

Figure S2. Cyclic voltammograms of DPPI-DBF, Cz-PPI-DBF and TPA-PPI-DBF.

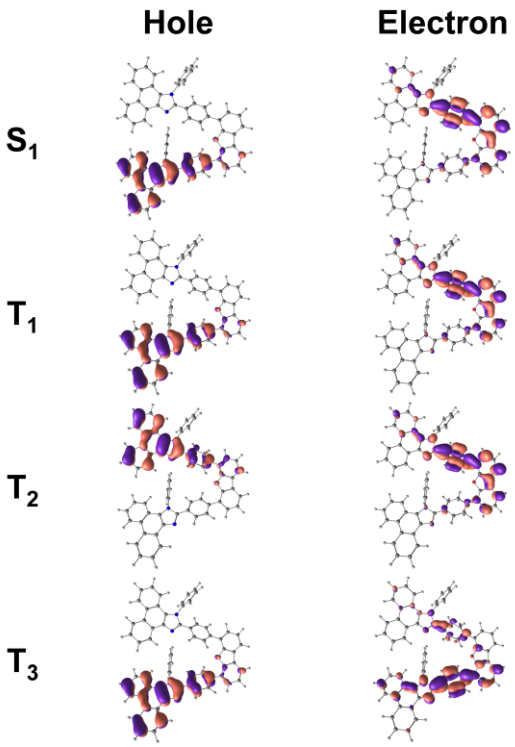

Figure S3. The calculated natural transition orbitals (NTOs) of DPPI-DBF.

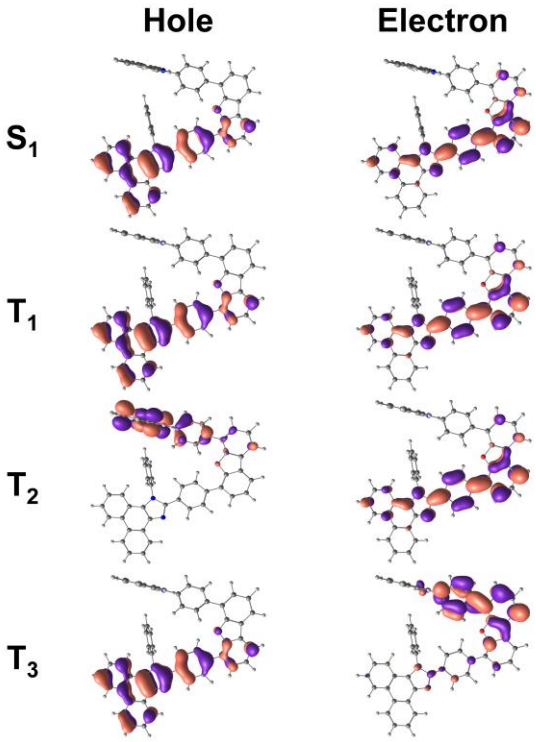

Figure S4. The calculated natural transition orbitals (NTOs) of Cz-PPI-DBF.

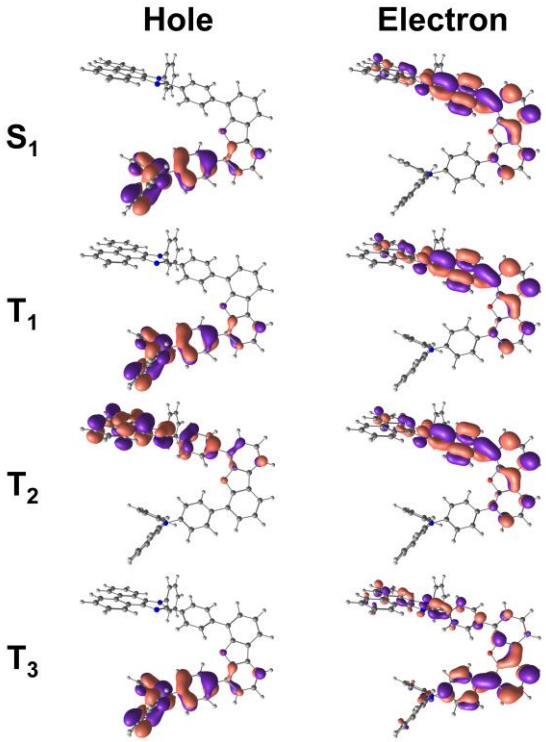

Figure S5. The calculated natural transition orbitals (NTOs) of TPA-PPI-DBF.

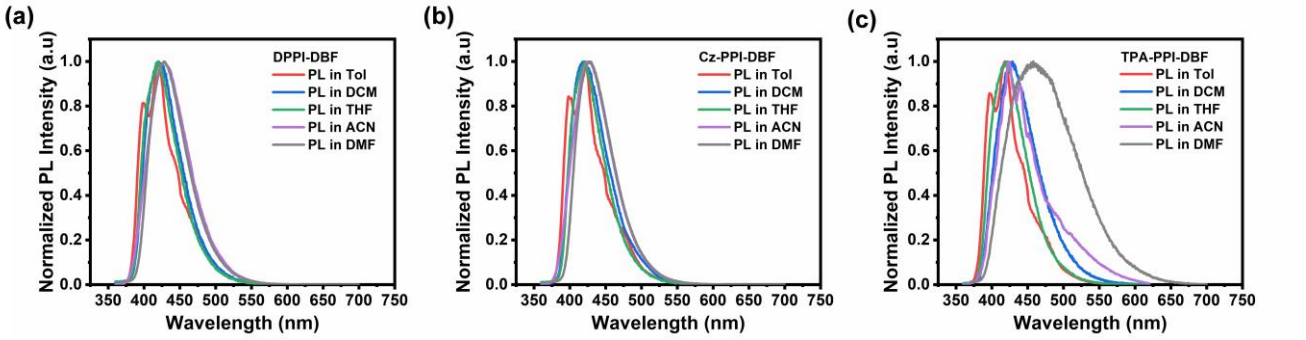

Figure S6. The PL spectrum of DPPI-DBF(a), Cz-PPI-DBF(b) and TPA-PPI-DBF(c) obtained in various solvents with increasing solvent polarity at room temperature..

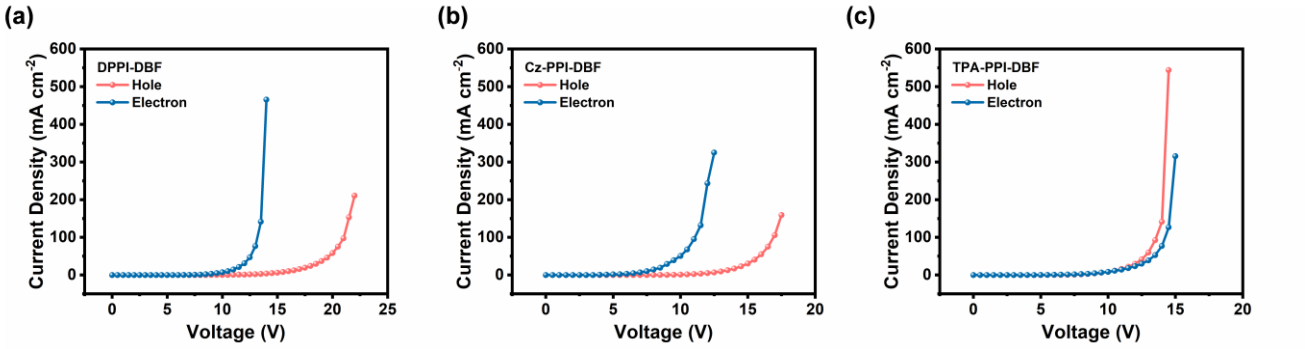

Figure S7. Current density - Voltage curves for the hole-only device (HOD) and the electron-only device (EOD) of DPPI-DBF(a), Cz-PPI-DBF(b) and TPA-PPI-DBF(c).

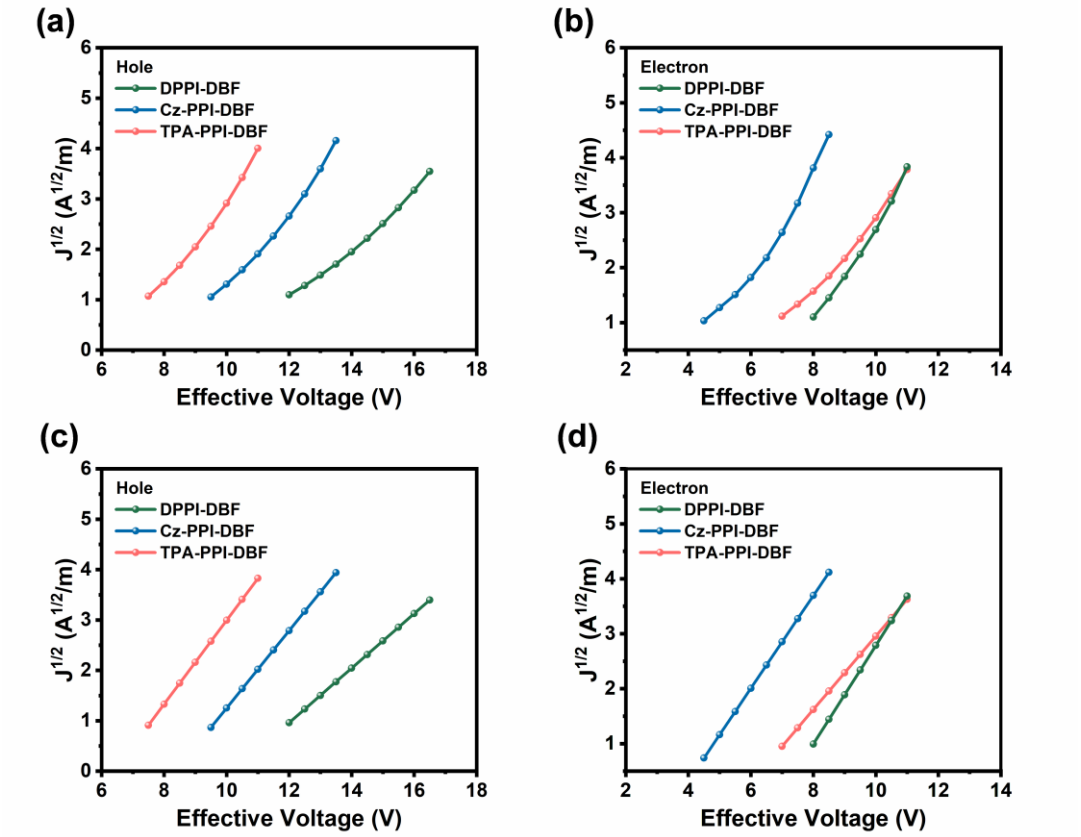

Figure S8. The $J^{1/2}$-V curves of single-carrier devices at the space-charge limited current district. The $J^{1/2}$-V curves of (a)Hole and (b) electron at effective voltage. The $J^{1/2}$-V fitting curves of (a) Hole and (b) electrons at effective voltage.

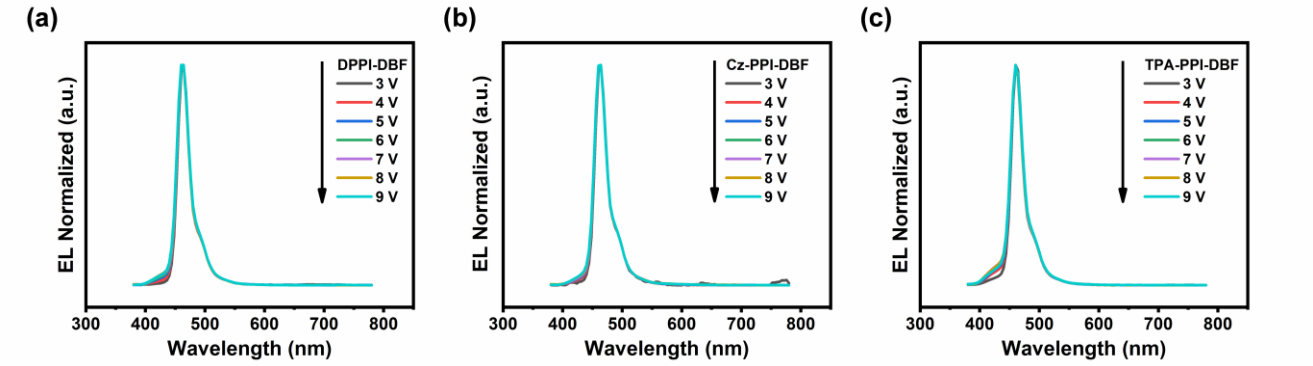

Figure S9. The EL spectrum at different voltage (3-9 V) of DPPI-DBF, Cz-PPI-DBF and TPA-PPI-DBF.

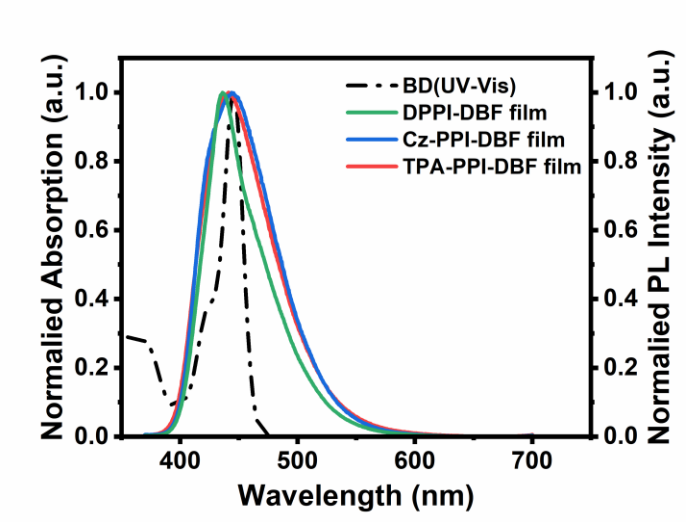

Figure S10. The UV-vis absorption of BD in the CH_2Cl_2 and pure thin film spectra of DPPI-DBF, Cz-PPI-DBF and TPA-PPI-DBF.

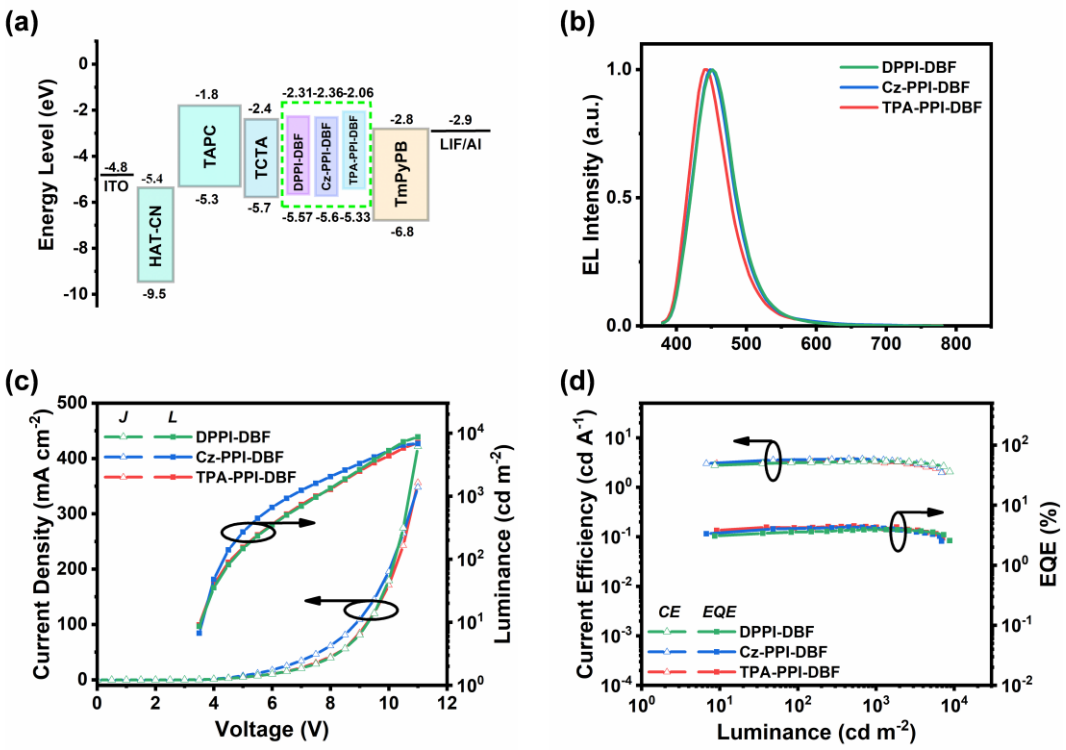

Figure S11. (a) Device structure. (b) The EL spectra of the devices. (c) The current density-voltage- luminance (J-V-L) curves of the devices. (d) The CE and EQE versus luminance relationships of the devices of DPPI-DBF, Cz-PPI-DBF and TPA-PPI-DBF.

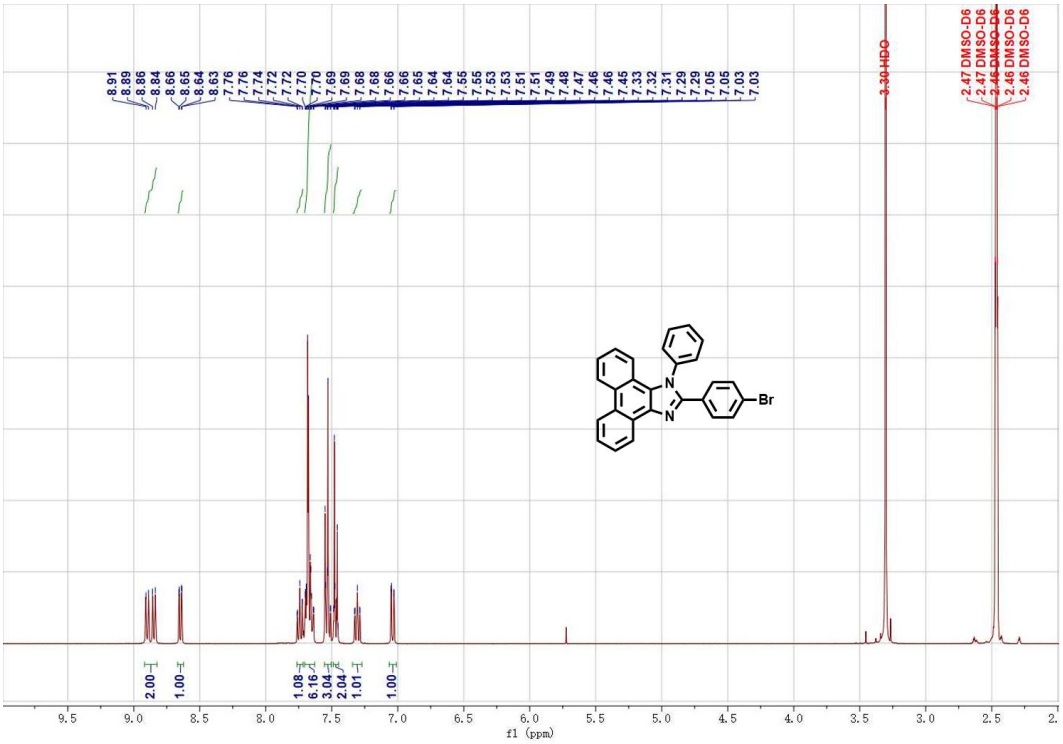

Figure S12. [1]H-NMR spectrum of compound **PPIBr** in deuterated DMSO-d6

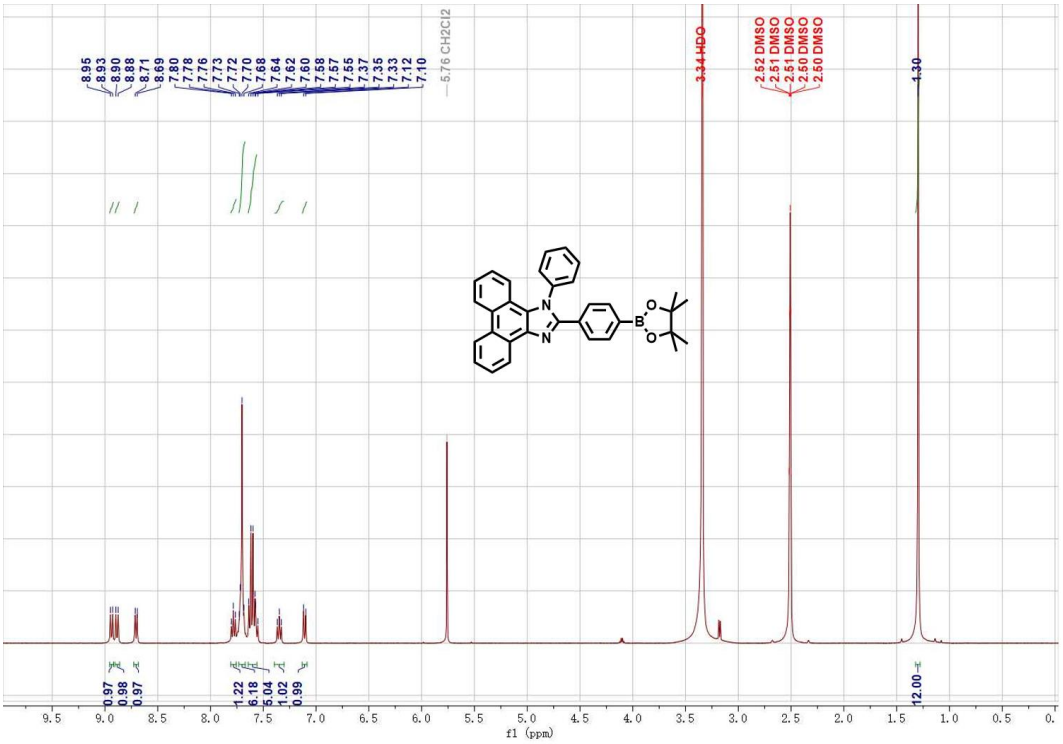

Figure S13. [1]H-NMR spectrum of compound **PPIBpin** in deuterated DMSO-d6

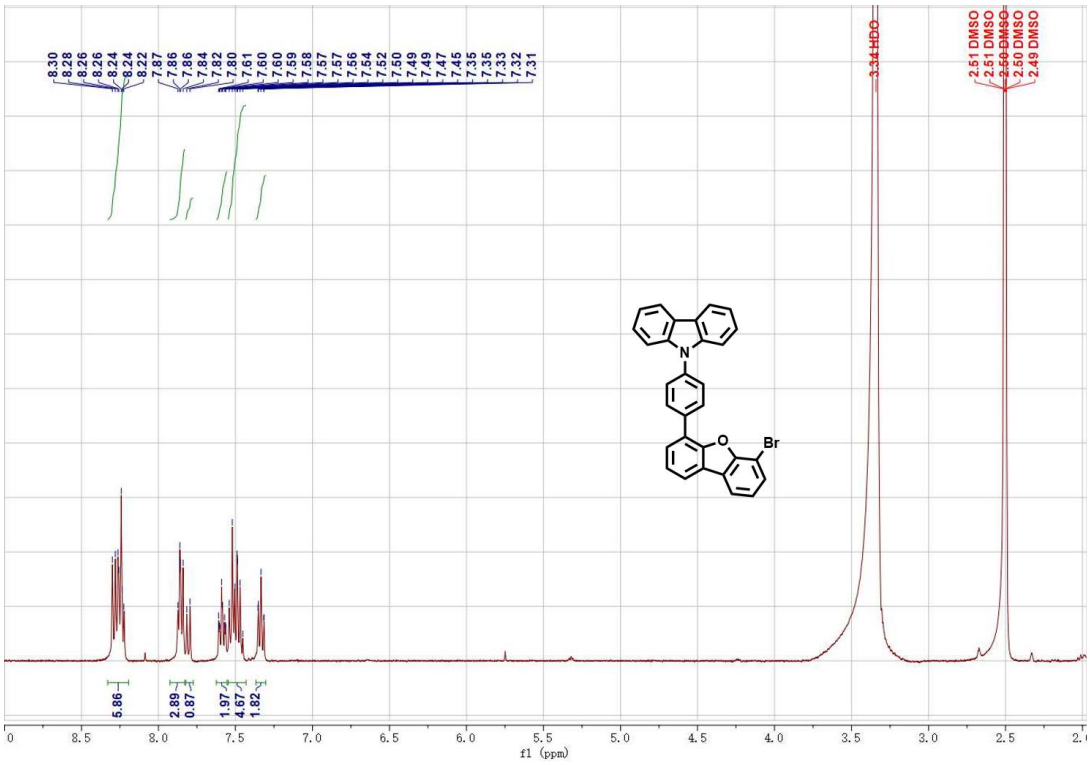

Figure S14. [1]H-NMR spectrum of compound **Cz-DBFBr** in deuterated DMSO-d6

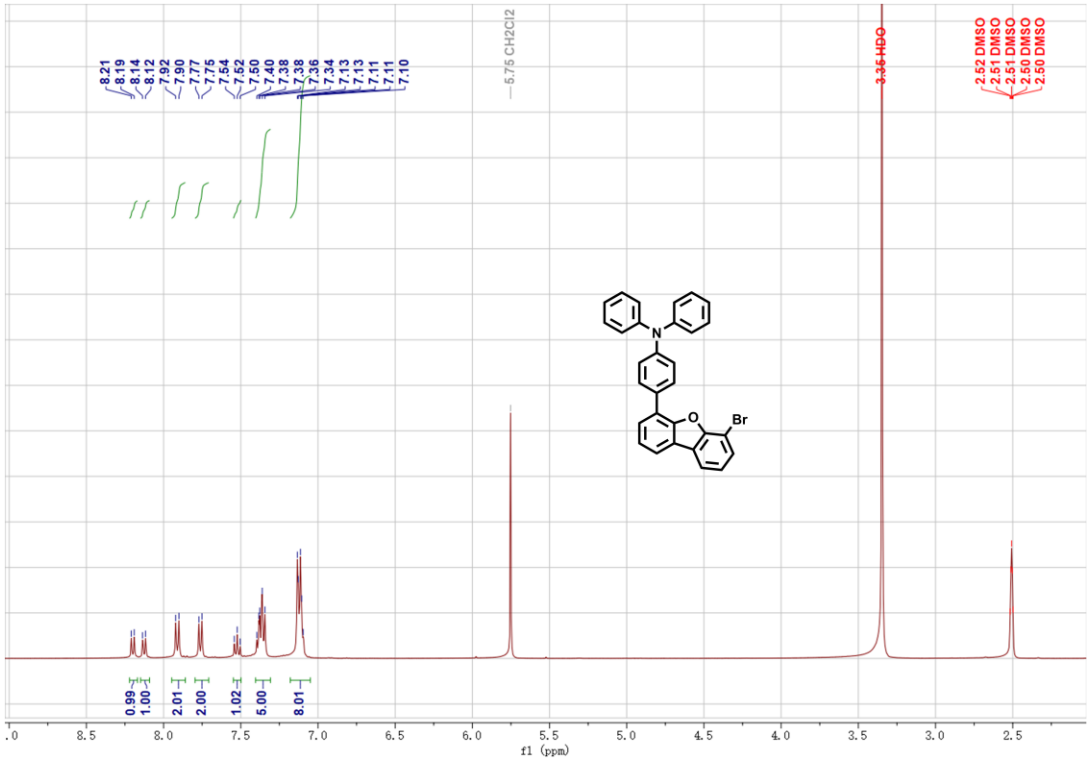

Figure S15. [1]H-NMR spectrum of compound **TPA-DBFBr** in deuterated DMSO-d6

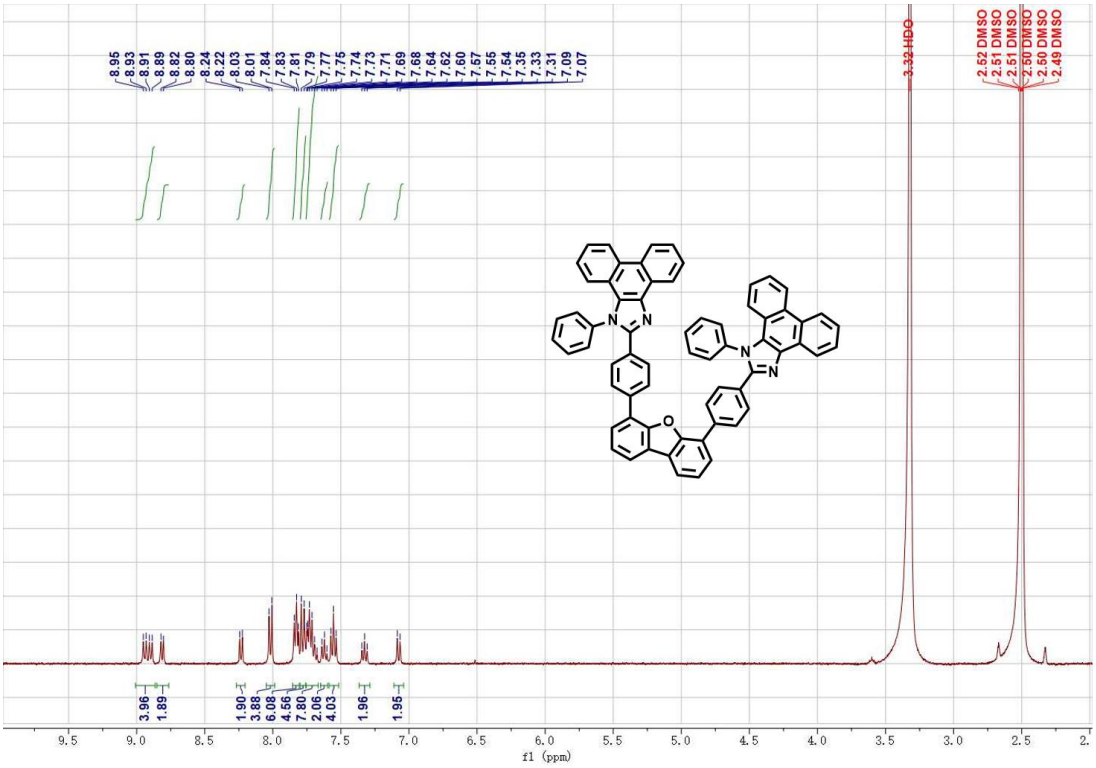

Figure S16. [1]H-NMR spectrum of compound **DPPI-DBF** in deuterated DMSO-d6

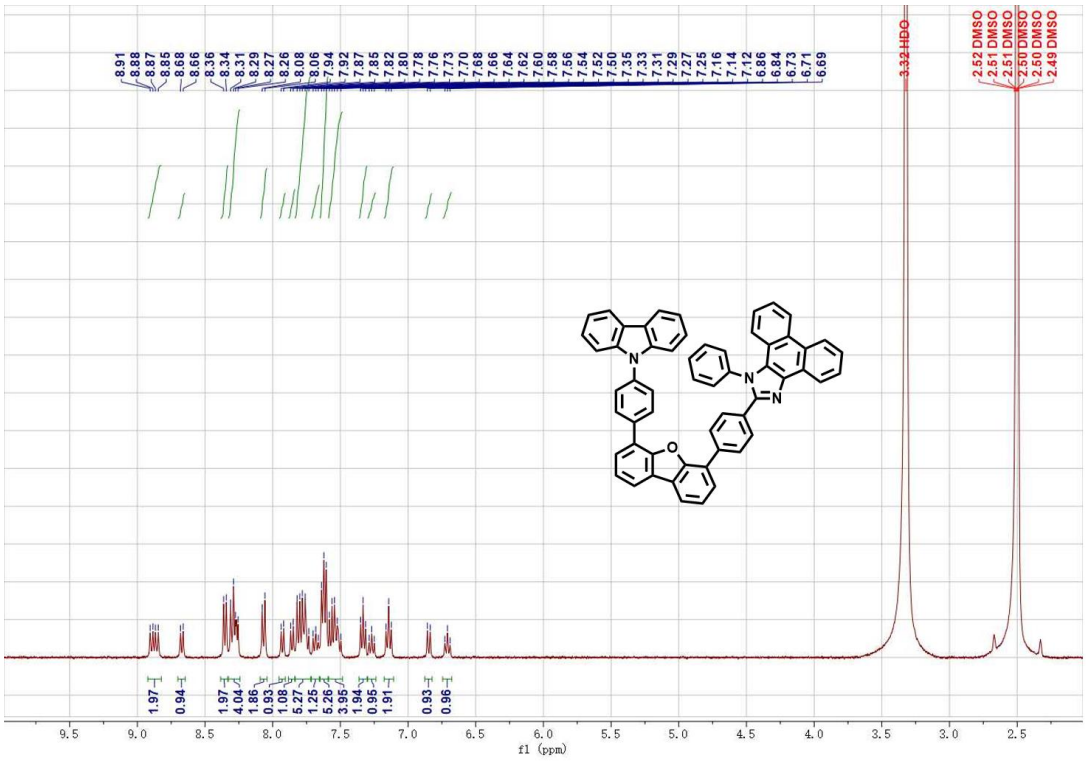

Figure S17. [1]H-NMR spectrum of compound **Cz-PPI-DBF** in deuterated DMSO-d6

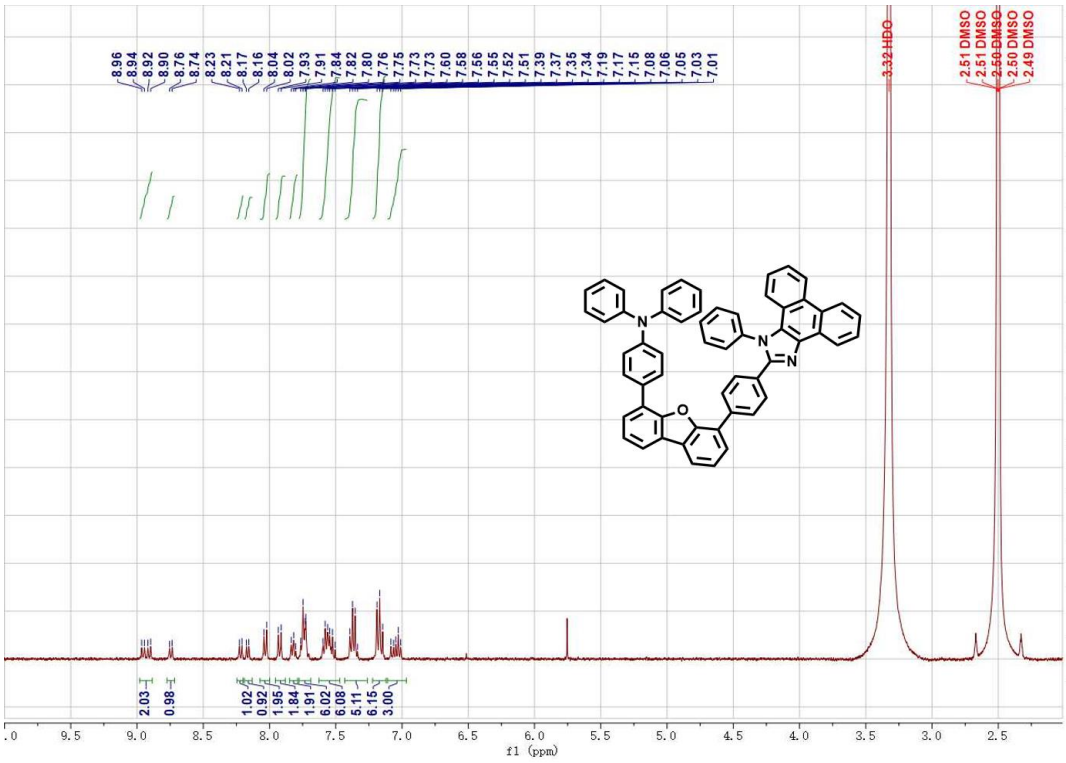

Figure S18. [1]H-NMR spectrum of compound **TPA-PPI-DBF** in deuterated DMSO-d6

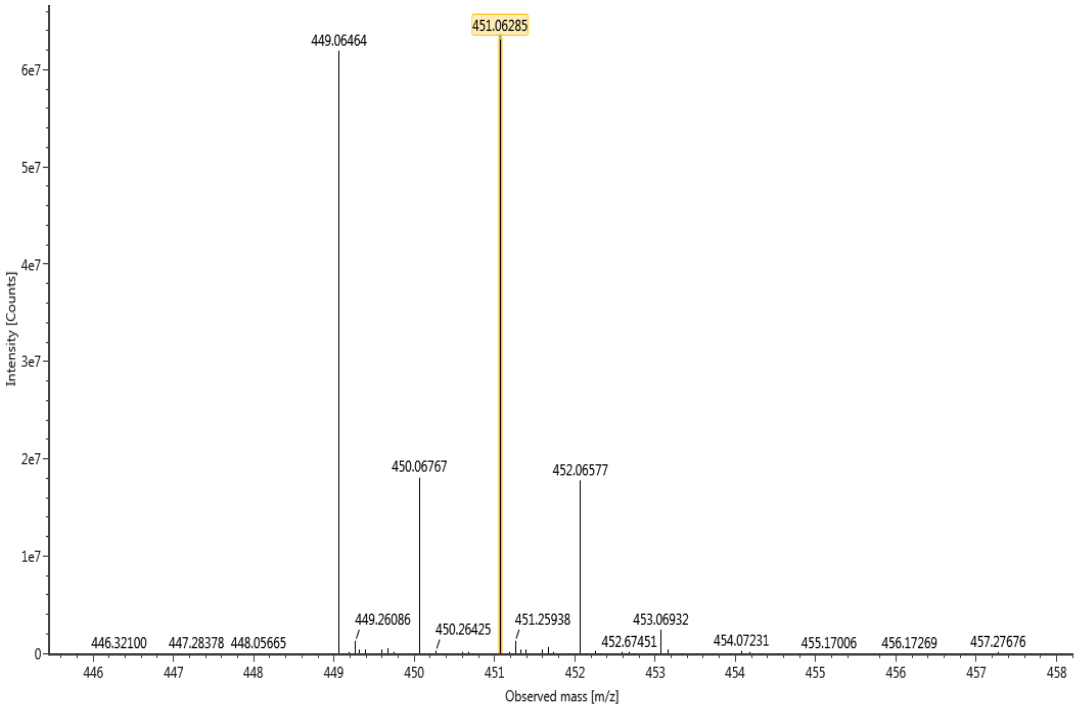

Figure S19. MS spectrum of **PPIBr**.

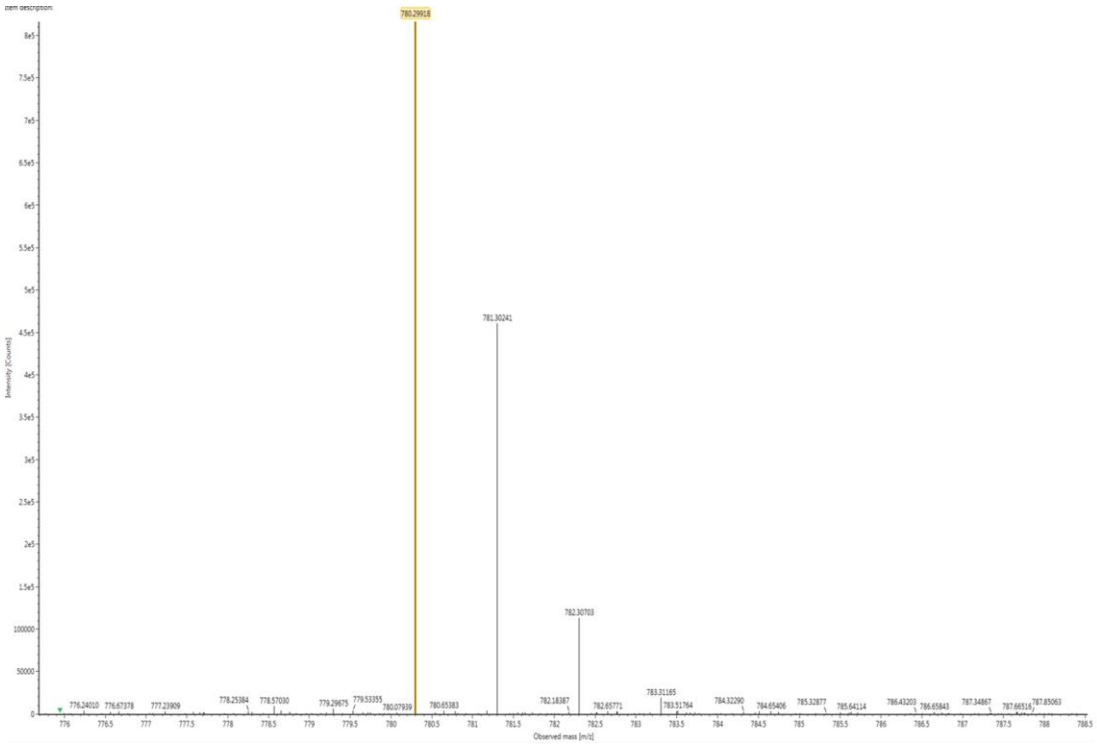

Figure S20. MS spectrum of **TPA-PPI-DBF**.

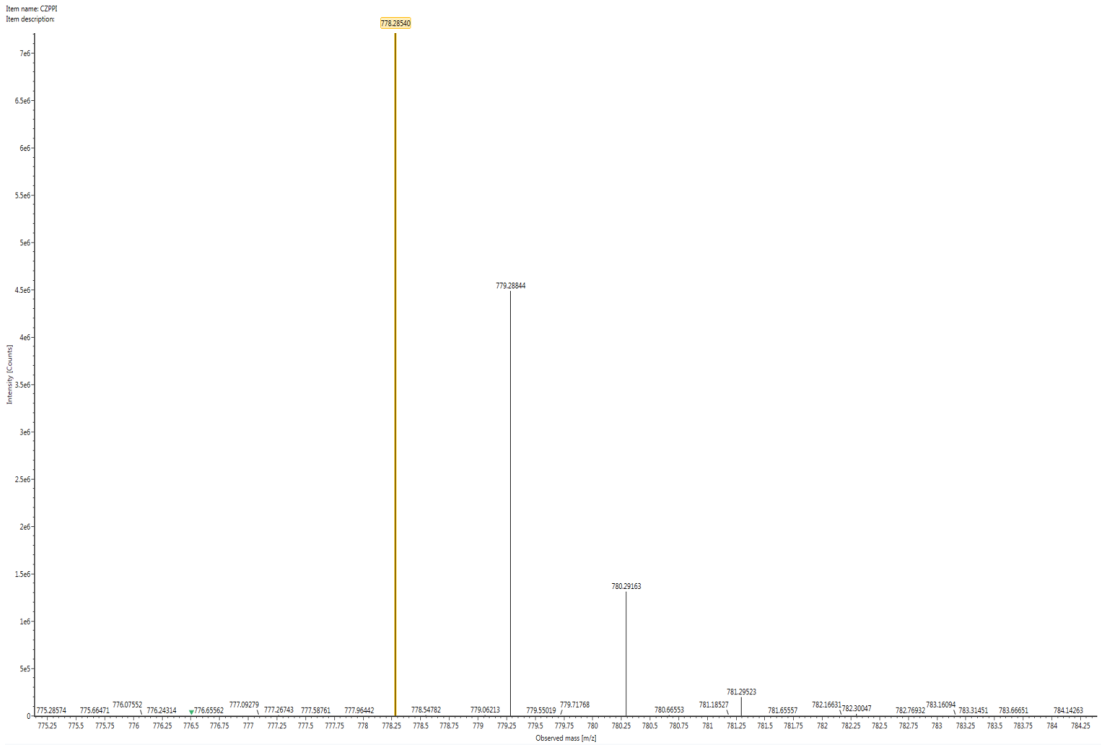

Figure S21. MS spectrum of **Cz-PPI-DBF**.

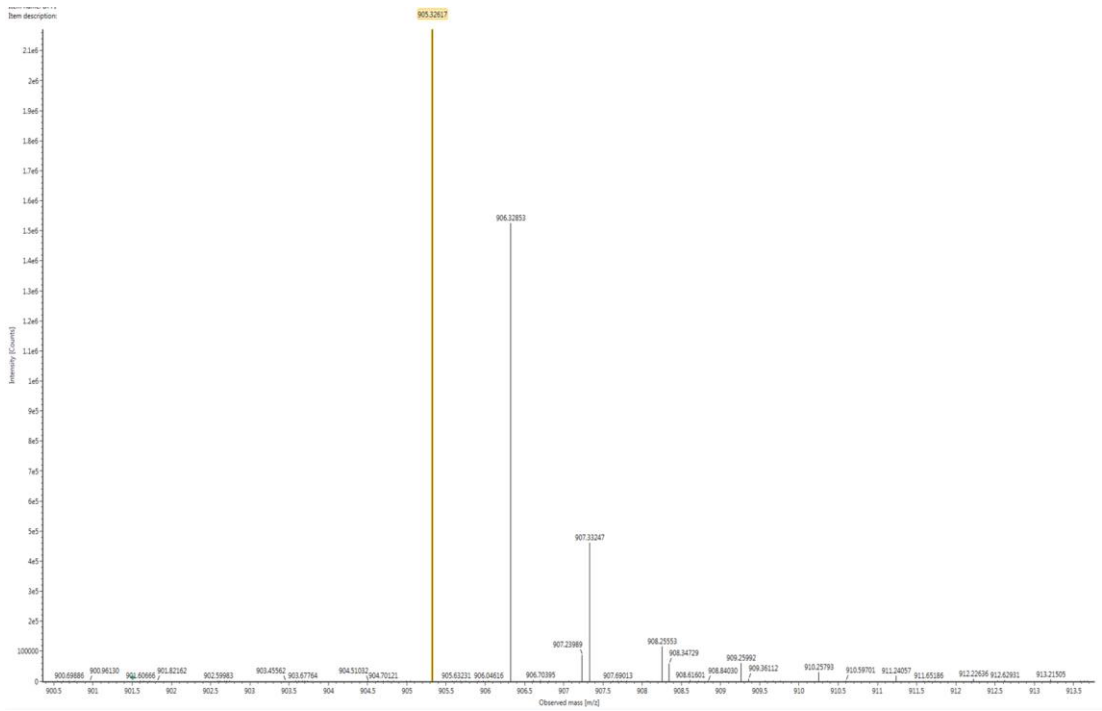

Figure S22. MS spectrum of **DPPI-DBF**.

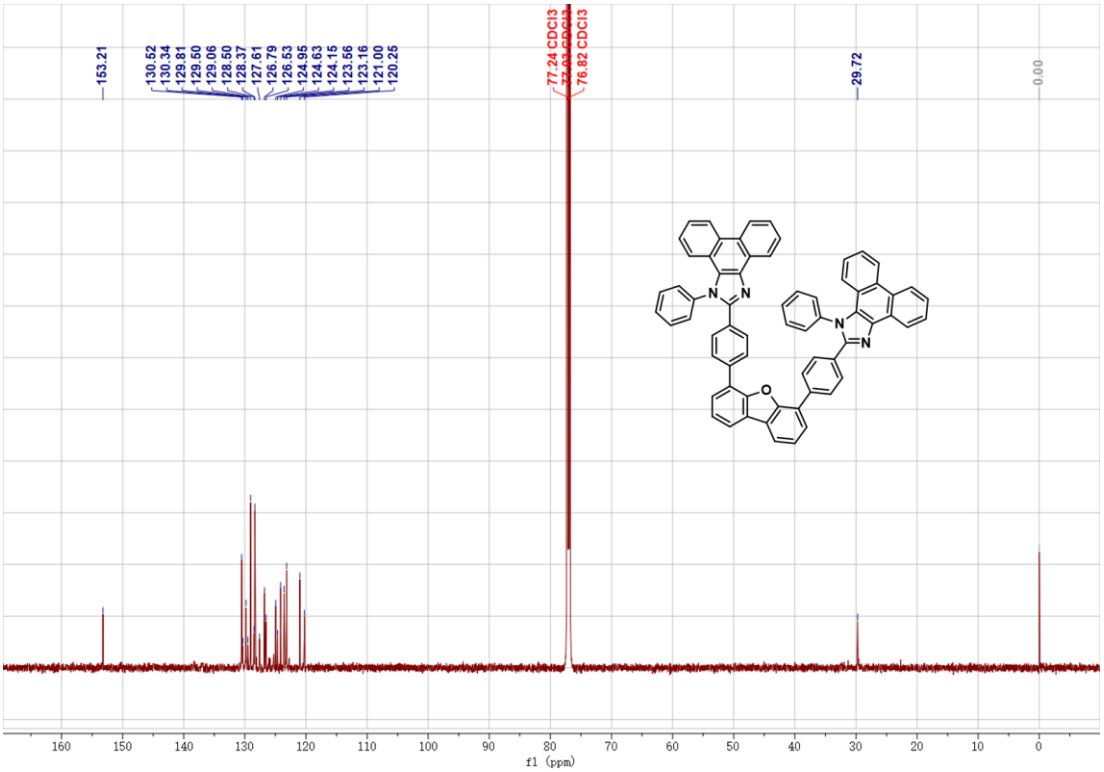

Figure S23. ^{13}C-NMR spectrum of compound **DPPI-DBF** in deuterated $CDCl_3$ solvent.

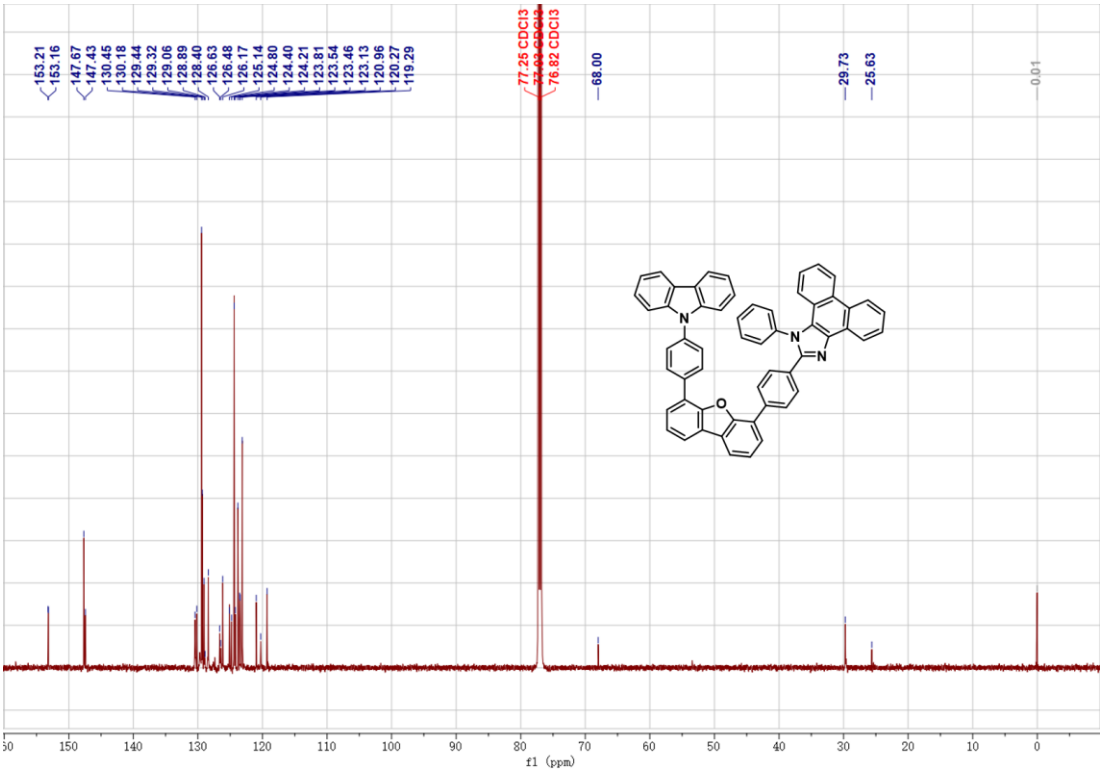

Figure S24. ^{13}C-NMR spectrum of compound **Cz-PPI-DBF** in deuterated $CDCl_3$ solvent.

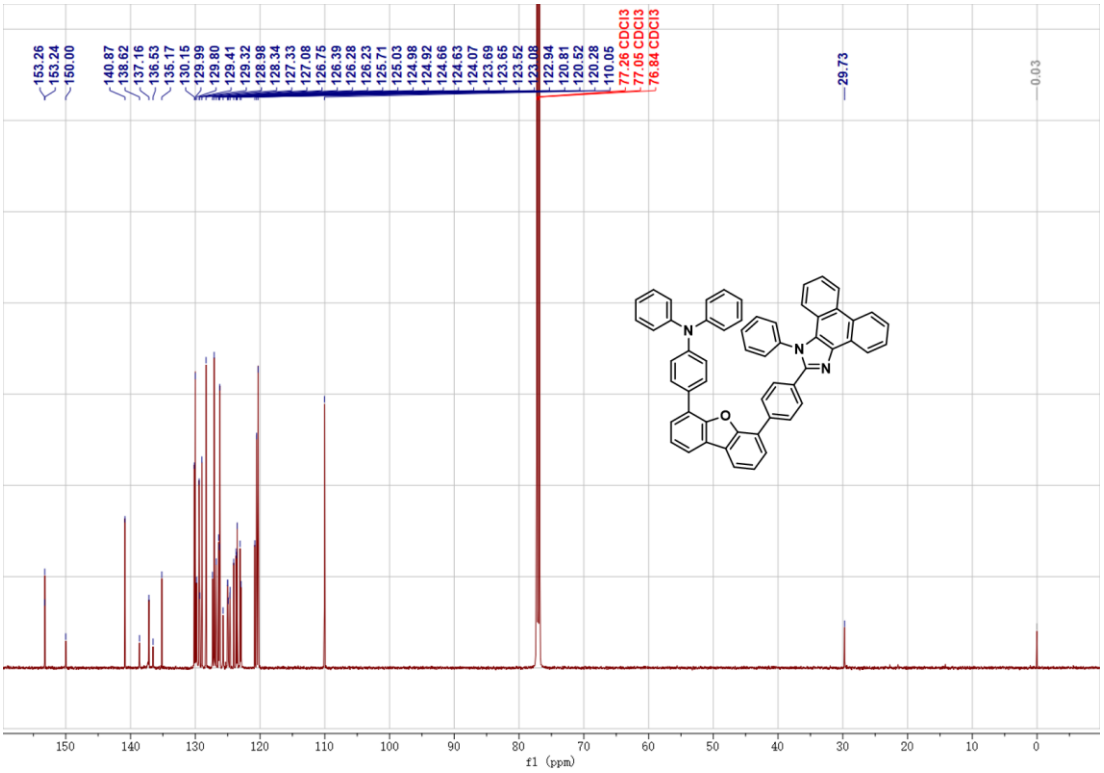

Figure S25. ^{13}C-NMR spectrum of compound **TPA-PPI-DBF** in deuterated $CDCl_3$ solvent.

S6. References

1. Gaussian 09, Revision A.02, M. J. Frisch, G. W. Trucks, H. B. Schlegel, G. E. Scuseria, M. A. Robb, J. R. Cheeseman, G. Scalmani, V. Barone, G. A. Petersson, H. Nakatsuji, X. Li, M. Caricato, A. Marenich, J. Bloino, B. G. Janesko, R. Gomperts, B. Mennucci, H. P. Hratchian, J. V. Ortiz, A. F. Izmaylov, J. L. Sonnenberg, D. Williams-Young, F. Ding, F. Lipparini, F. Egidi, J. Goings, B. Peng, A. Petrone, T. Henderson, D. Ranasinghe, V. G. Zakrzewski, J. Gao, N. Rega, G. Zheng, W. Liang, M. Hada, M. Ehara, K. Toyota, R. Fukuda, J. Hasegawa, M. Ishida, T. Nakajima, Y. Honda, O. Kitao, H. Nakai, T. Vreven, K. Throssell, J. A. Montgomery, Jr., J. E. Peralta, F. Ogliaro, M. Bearpark, J. J. Heyd, E. Brothers, K. N. Kudin, V. N. Staroverov, T. Keith, R. Kobayashi, J. Normand, K. Raghavachari, A. Rendell, J. C. Burant, S. S. Iyengar, J. Tomasi, M. Cossi, J. M. Millam, M. Klene, C. Adamo, R. Cammi, J. W. Ochterski, R. L. Martin, K. Morokuma, O. Farkas, J. B. Foresman, and D. J. Fox, Gaussian, Inc., Wallingford CT, 2016.

2. J. Zheng , X. Xu and D. G. Truhlar , Theor. Chem. Acc., 2010, 128 , 295 - 305.

3. J. Yang , Z. Ren , Z. Xie , Y. Liu , C. Wang , Y. Xie , Q. Peng , B. Xu , W. Tian , F. Zhang , Z. Chi , Q. Li and Z. Li , Angew. Chem., Int. Ed., 2017, 56 , 880-884.

4. F. Neese: Software update: the ORCA program system, version 4.0 (WIREs Comput Mol Sci 2018,8:e1327.